3D Printing of Conjugated Polymers

Robert S. Jordan, Yue Wang

Department of Materials Science and Engineering, University of California, Merced, Merced, California 95343
Correspondence to: Y. Wang (E-mail: yuewang@ucmerced.edu)

Received 22 June 2019; revised 27 September 2019; accepted 27 September 2019; published online 23 October 2019
DOI: 10.1002/polb.24893

ABSTRACT: Three-dimensional (3D) printing brings exciting prospects to the realm of conjugated polymers (CPs) and organic electronics through vastly enhanced design flexibility, structural complexity, and environmental sustainability. However, the use of 3D printing for CPs is still in its infancy and remains full of challenges. In this review, we highlight recent studies that demonstrate proof-of-concept strategies to mitigate some of these problems. Two general additive manufacturing approaches are featured: direct ink writing and vat photopolymerization. We conclude with an outlook for this thriving field of research and draw attention to the new possibilities that 3D printing can bring to CPs. © 2019 Wiley Periodicals, Inc. J. Polym. Sci., Part B: Polym. Phys. **2019**, *57*, 1592–1605

KEYWORDS: 3D printing; additive manufacturing; conjugated polymers; digital light processing; direct ink writing; polymer processing; stereolithography

INTRODUCTION Ever since the 1977 discovery that doped polyacetylene is highly conducting, conjugated polymers (CPs) have dramatically evolved from scientific curiosities to materials with commercial success.[1,2] Organic light emitting diodes (OLEDs) and organic photovoltaics (OPV) are but two shining examples.[3–6] Despite their inferior mobility and conductivity compared to their inorganic counterparts such as silicon and copper, CPs have become a serious contender in the electronics and optoelectronics industry largely due to their synthetically tunable properties and solution processability.[7,8] In particular, the low cost and near room temperature solution processing methods are attractive properties for consumer electronics.[9]

The unique chemical, physical, and processing properties of CPs have also made them competitive contenders for next-generation wearable or implantable electronics.[9,10] Such applications require electronic devices to be stretchable to accommodate the three-dimensional (3D) movement of the human body while maintaining electrical performance. Most of the solution processing methods developed for CPs for OPV, OLED, or organic field-effect transistors (OFETs) applications (Fig. 1) can be applied to the fabrication of wearable and epidermal organic electronics.[11] Common approaches such as spin coating, drop casting, blade coating, and spray coating, are among a variety of direct printing and meniscus-guided coating methods.[12] Virtually all of these methods rely on processing the CPs onto a two-dimensional (2D) substrate, followed by stretching the device onto the human skin,[10] which has a 3D topography. Bridging this gap in 2D processing and 3D applications can potentially render this class of materials equally, or even more, competitive than inorganic materials in the booming field of wearable and epidermal electronics. 3D printing has therefore become the popular choice for bridging this gap in dimensionality. Furthermore, the design flexibility offered by 3D printing can create new opportunities for CPs in other applications, such as bioelectronics that can be personalized for each individual, free-form energy harvesting or storage devices that can take advantage of unused gap spaces, as well as prosthetic devices with lightweight, functional electronic components.

3D printing, a subfield of additive manufacturing (AM), has quickly captivated scientists and engineers from all disciplines because of the geometric freedom and complexity that it can offer (Fig. 2).[13] The additive nature of the technique also renders it more environmentally friendly than the wasteful, subtractive, lithography-based processing and patterning methods currently used for the fabrication of most electronics. These features are attractive for applications in virtually all areas of science and engineering, including load-carrying parts in the automobile and aerospace industries, personalized prosthetics, tissue engineering, electronics, mechanical metamaterials, soft robotics, optics, and bioinspired materials.[14]

Despite these alluring prospects, reports on 3D printing of CPs are scarce. In this review, we will start by providing an overview of the most commonly used 3D printing methods and discuss the materials and machine building challenges for processing CPs using these tools. We will then survey the current status of the field and highlight two specific 3D printing techniques, direct ink writing (DIW) and vat

Robert S. Jordan obtained his B.S. degree in Chemistry from Occidental College in 2010. In 2017, he received his Ph.D. from the University of California, Los Angeles under the direction of Yves Rubin developing novel synthetic approaches to graphene nanoribbons. Robert is currently a Postdoctoral Scholar at the University of California, Merced with Yue Wang. His research interests include the synthesis of tailored conjugated molecules and their spectroscopic investigation, as well as additive manufacturing for organic electronics.

Yue Wang received her B.S. degree in Chemistry and Ph.D. in Inorganic Chemistry in 2008 and 2014, respectively, working with Richard B. Kaner on organic single crystals at the University of California, Los Angeles. She also carried out research on transparent conductors as a staff researcher at Fibron Technologies, Inc., in the years 2008–2009. She was a postdoctoral fellow with Zhenan Bao at Stanford University between 2014 and 2017 working on stretchable electronics. She is currently an assistant professor of Materials Science and Engineering at the University of California, Merced. Her research group focuses on bioinspired organic electronic materials and uses three-dimensional printing to realize complex hierarchical structures inspired from nature.

photopolymerization [which includes stereolithography apparatus (SLA) and digital light processing (DLP)], that are uniquely suited to be compatible with CPs. Finally, we will conclude with an outlook highlighting opportunities and challenges. We hope this review can (a) excite researchers in the CP community to explore 3D printing techniques as new processing methods for next-generation organic electronics, and (b) ignite interest in researchers from the 3D printing community to build machines that are tailored toward processing CPs, and potentially add these unique polymers to their standard material repertoire.

CHALLENGES FOR 3D PRINTING CONJUGATED POLYMERS

In order to overcome challenges in processing a material via a given approach, we need to first develop an understanding of the processing method itself. Therefore, we start this section by providing an overview of the commonly used 3D printing methods, and then move on to the specific challenges in 3D printing of CPs.

3D Printing Methods

Within the field of AM, Chuck Hull is widely regarded as the "father" of 3D printing due to his pioneering patent for the first AM technique submitted in 1984.[15,16] The term SLA was first disclosed within Hull's patent application, but the roots of the technique can be traced back to experiments carried out by Hideo Kodama in 1981 at the Nagoya Municipal Research Institute.[17] While the first commercial SLA printers were developed in the 1980s by 3D systems, today, there exists a large range of AM instruments for the professional or the hobbyist. The three most widely utilized AM techniques

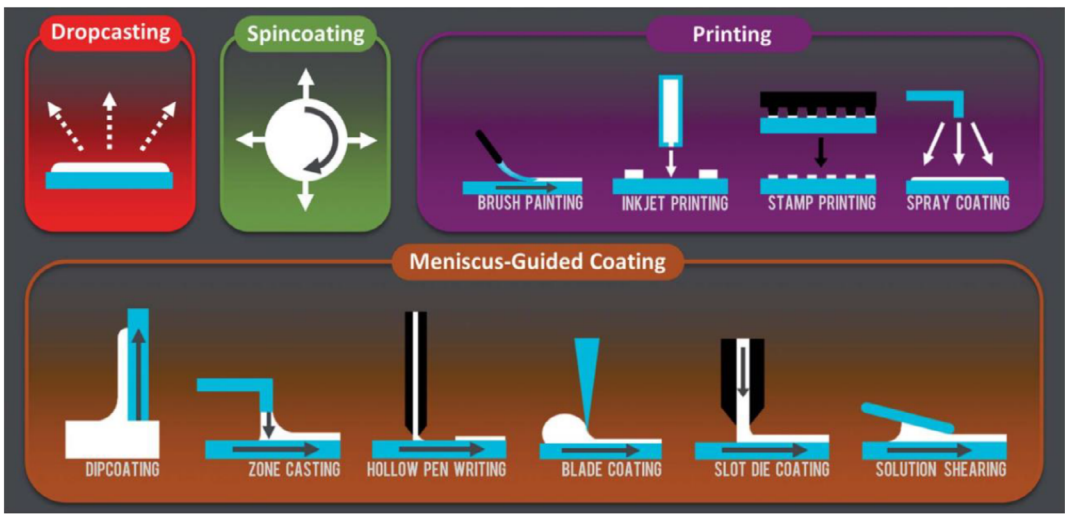

FIGURE 1 An overview of solution-based 2D deposition techniques for CPs. (Reproduced from ref. 11, published by the Royal Society of Chemistry under the Creative Commons Attribution 3.0 Unported License (creativecommons.org/licenses/3.0).) [Color figure can be viewed at wileyonlinelibrary.com]

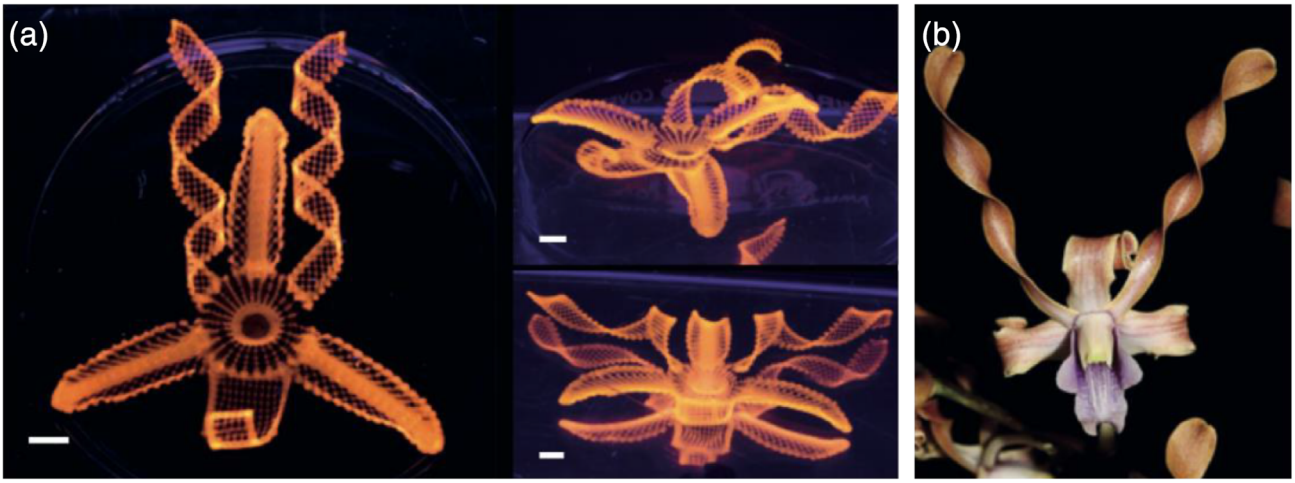

FIGURE 2 An example of a 3D printed object to demonstrate the resolution and complexity achievable by this processing method. (a) Orchids printed using an extrusion-based method that display high complexity and anisotropic swelling which produce twisted structures that mimic nature. (b) The orchid *Dendrobium helix* which served as the basis for the print (scale bars, 5 mm). (Reproduced from ref. 13, with permission from the Nature Publishing Group.) [Color figure can be viewed at wileyonlinelibrary.com]

are (a) fused deposition modeling (FDM), also known as melt material extrusion, (b) stereolithography and the closely related DLP (collectively known as vat photopolymerization), and (c) selective laser sintering (SLS) [Fig. 3(a,d,e)].[18,19] In FDM, a filament comprised of a thermoplastic such as poly(lactic acid) or acrylonitrile–butadiene–styrene is heated above its glass transition temperature (T_g) so that the material can flow out of the nozzle and be deposited onto a heated substrate in layers to provide the 3D structure [Fig. 3(a)]. Due to its simplicity and low material cost, FDM printers have become the most widely used hobbyist 3D printing technique. SLA and DLP both utilize an ultraviolet (UV) light source (typically 405 nm) to selectively cure a 2D pattern into a thin layer of a photoreactive resin [Fig. 3(e)]. Addition of a fresh layer of resin followed by curing allows 3D structures to be produced from digitally controlled light patterns. SLS can produce both plastic and metal parts, but the fundamental process is the same regardless of the material to be printed. A thin layer of material in the form of a fine powder is heated locally using a focused beam of laser light. Local heating causes the particle within the beam to sinter and form a solid object [Fig. 3(d)]. After a 2D pattern has been created, a fresh layer of powder is added and the process repeated until the desired object is formed. For those who are interested in the detailed mechanisms and examples of 3D printing, we refer the reader to the following references for information.[14,20]

Challenges and Opportunities for 3D Printing CPs

When choosing a 3D printing technique to use with CPs, polymer stability is of significant importance. In both FDM and SLS, the materials to be deposited/molded are heated above their glass transition temperature or melting point. Due to the electron-rich nature of CPs, many of these materials undergo irreversible oxidation/decomposition upon prolonged exposure to oxygen, and this effect is typically accelerated via heating.[21–23] This chemical instability makes adaption of this

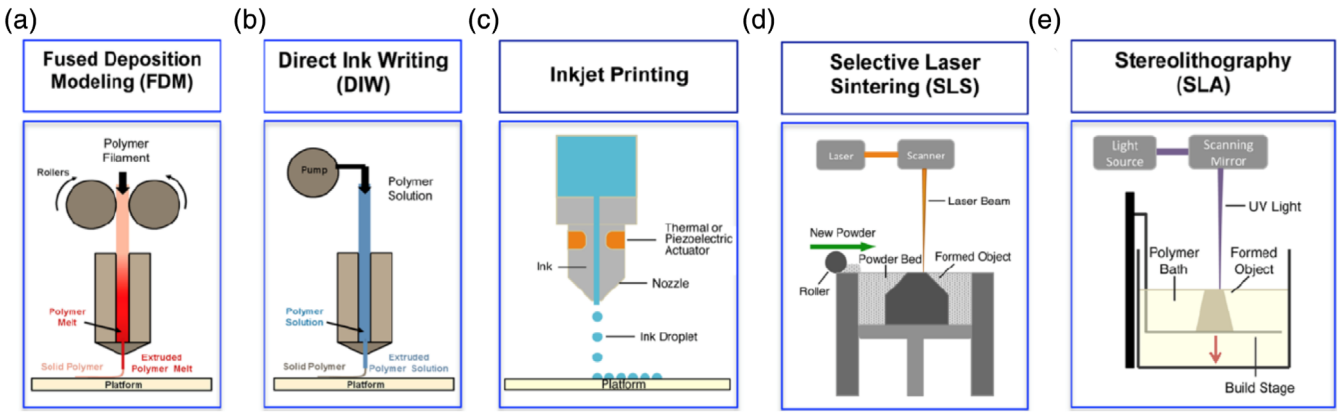

FIGURE 3 Schematics depicting 3D printing techniques: extrusion-based methods such as FDM (a) and DIW (b), inkjet printing (c), particle fusion-based methods such as SLS (d), and light-based method SLA (e). (Reproduced from ref. 18, with permission from the American Chemical Society.) [Color figure can be viewed at wileyonlinelibrary.com]

class of polymers to 3D printing particularly challenging. However, one of the attractive features of CPs is that they can be made solution processable through a diverse array of chemistries and techniques. Careful synthetic design allows for the incorporation of solubilizing side chains onto the CP backbone, which can offer exquisite control over the solution processing conditions of a CP.[5,24,25] Many CPs that are not fully soluble can be processed as dispersions, allowing material deposition using nozzle-based 3D printing techniques such as DIW. We will discuss representative studies in the Direct Ink Writing section.

Another beneficial feature of CPs for their incorporation into 3D printing is that they are synthesized bottom-up from monomers or oligomers. SLA/DLP 3D printing is based on photopolymerization of a reactive resin. Although direct photopolymerization of CPs is rare, clever design of resin systems using a cascade of reactions can afford the direct synthesis of some of these polymers under the irradiation of light. We will discuss representative studies on the SLA/DLP 3D printing on CPs in the Vat Photopolymerization Techniques: SLA and DLP section. Many CPs also display electromechanically active behavior with their electrical properties (typically resistance) changing under applied stress. This can be exploited to create a number of useful devices such as actuators, sensors, or the direct harvesting of mechanical energy through this behavior. A recent publication has described 3D printed CP systems which displays such behavior.[26]

We focus on conducting polymers instead of semiconducting polymers in this review as they are the subject of virtually all existing reports on 3D printing of CPs, principally due to their ease of synthesis and potential for practical applications in the near term.

ADDITIVE MANUFACTURING OF CONJUGATED POLYMERS

2D Additive Manufacturing of CPs

Before we begin our discussion of DIW and SLA/DLP, we would like to briefly discuss the technique of inkjet printing (IJP), a well-investigated AM method for 2D structures. Of the additive techniques, printing with CPs has seen the most development utilizing IJP. The major limitation of this technique is the difficulty in translating 2D patterns formed by IJP into genuine 3D structures, and to date this has not been resolved concerning CPs. We will discuss the reasons for this limitation, but first, we give a brief overview of the development of printing CPs utilizing IJP.

As a technique, IJP has been under constant development for decades, with the printing of CPs having been first reported in the late 1990s.[27] Since the initial reports, IJP of conjugated materials has seen a wealth of publications and been the subjects of recent reviews.[28,29] In general, IJP has proven to be a reliable and robust technique for the formation of complex 2D patterns with low-viscosity inks (typically <100 cP). Its additive nature, where patterning is completed during the processing step, renders this method more environmentally friendly and cost-effective than the other commonly used methods, such as spin coating or drop casting. As noted earlier, the tunable solubility of CPs makes them ideal for incorporation into IJP inks. For polymers with low or problematic solubility, methods have also been developed for the deposition of monomers via IJP followed by a postdeposition polymerization to form CPs.[30] Due to the inherent "2D" nature of most organic electronics to date (e.g., OPV, OLED), IJP has been utilized for the fabrication of organic electronics containing CPs and is relatively well developed. As an example, in nearly all organic electronics, careful control of polymer chain alignment is essential for good device performance.[31] Recent development has led to IJP processes that allow for manipulation of polymer chain alignment, enabling the printing of devices with anisotropic properties (Fig. 4).[32]

Despite the wealth of interest and progress made concerning the IJP of CPs, controlled layering of printed layers into the third dimension remains difficult. The major limitation keeping IJP of CPs from expanding to the third dimension is curing. Conventionally, most layers printed by IJP (CP and most other polymers) are cured not by chemical crosslinking, but by simple evaporation of the solvent. This produces a dried layer that is subject to redissolution and flow upon deposition of fresh ink. Industrially for non-conjugated materials, this problem has been solved by incorporation of UV-reactive inks into IJP technologies, such as the PolyJet system by Stratasys. The PolyJet system operates via IJP of mixtures of UV-curable resins allowing for the combination of multiple colors and materials within a single monolithic print. Taking inspiration from the PolyJet technology, it may be possible to develop IJP inks that contain CPs and UV-reactive crosslinkers that do not negatively affect the electrical properties of CPs. These mixed systems could provide IJP of CPs the breakthrough it needs to get to the third dimension.

We will now begin our discussion of two techniques that can currently create 3D structures containing CPs, DIW, and vat photopolymerization (SLA/DLP).

3D Printing of CPs

Direct Ink Writing

The origin of the DIW technique (also referred to as "Robocasting") is attributed to work performed in 1996 at Sandia National Laboratories.[33] The technique was initially developed for the deposition of inorganic slurries to create composites with complex 3D architectures. Recently, the technique has seen an explosion of use within research groups for the deposition of inorganic, organic, and biomaterials.[18,34] Typical DIW setups utilize a number of common extrusion strategies, including pneumatic or mechanical pistons and Archimedes screws (augers), depending on the application and material to be utilized (Fig. 5).[35] Attachment of these extruders to a commercially available 3D printer allows a low-cost DIW setup to be created for less than $1000. Some unique advantages of DIW are its low cost, ability to work with inks/pastes with a wide range of viscosities, and construction of complex structures without the need for lithographic techniques.

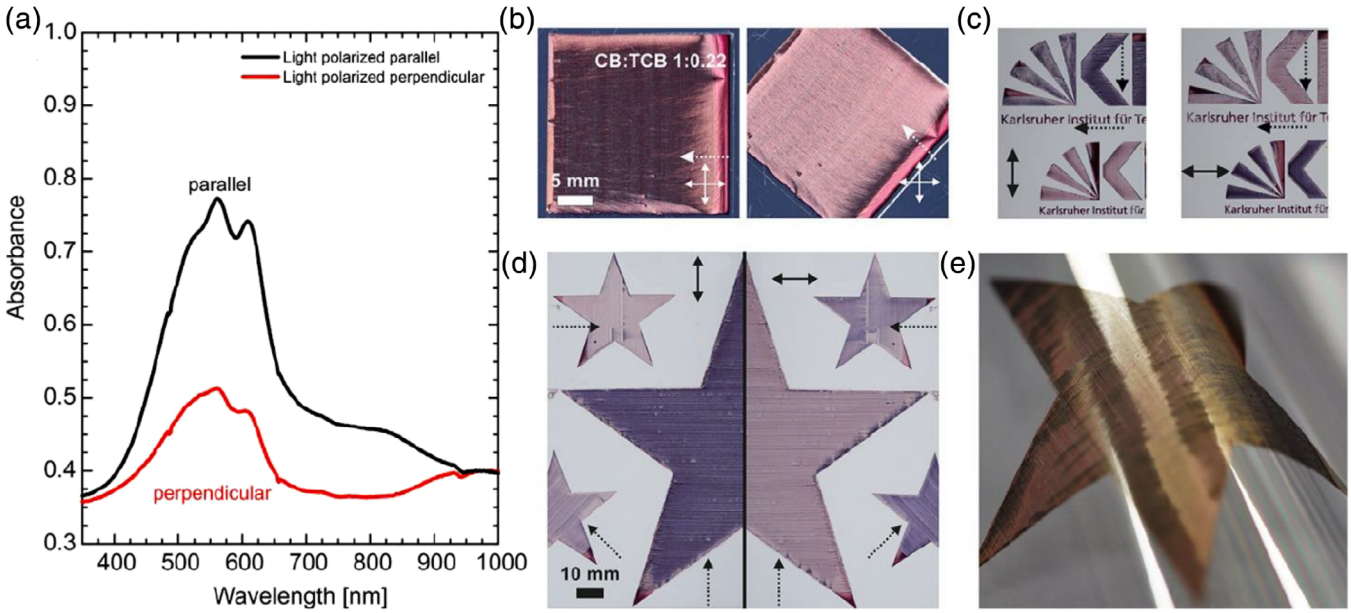

FIGURE 4 IJP processing and patterning of P3HT. (a) Absorbance spectra of aligned P3HT fibers with light source being polarized parallel or perpendicular to the fibers. (b) Crossed-polarized and polarized images of printed P3HT fibers; solid arrows indicate the orientation of the polarizers, and dashed arrows point in the printing direction. (c,d) Images of star-shaped printed P3HT fibers taken with polarizer; polarizer orientation is indicated by the solid arrow, and the printing direction is indicated by dashed arrows. (e) Photograph of fibers on flexible PET. (Reproduced from ref. 31, with permission from the American Chemical Society.) [Color figure can be viewed at wileyonlinelibrary.com]

Arguably, the most important aspect controlling the success of a DIW implementation is the rheology of the ink to be printed (Fig. 6). If the ink to be deposited has a relatively low viscosity and displays near-Newtonian properties, the ink is more suitable for IJP with deposition occurring in a drop-wise

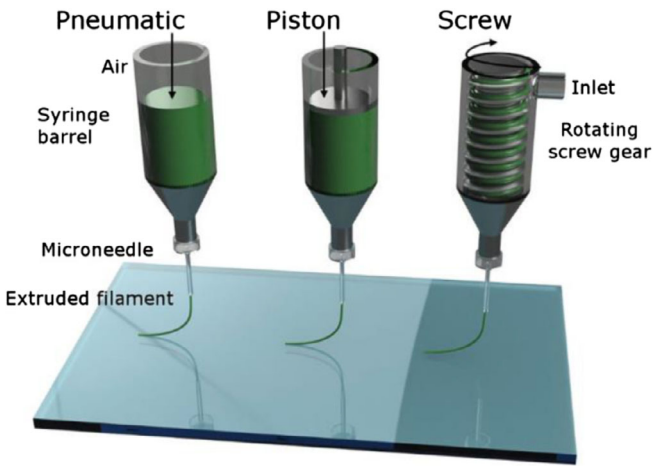

FIGURE 5 Comparison of nozzle-based extrusion strategies commonly utilized in DIW. The strategies differ in the mechanism by which the material is forced through the nozzle either by air (pneumatic), a piston, or a screw gear (auger). (Adapted from ref. 18, under the Creative Commons Attribution License (http://creativecommons.org/licenses/by/4.0)). [Color figure can be viewed at wileyonlinelibrary.com]

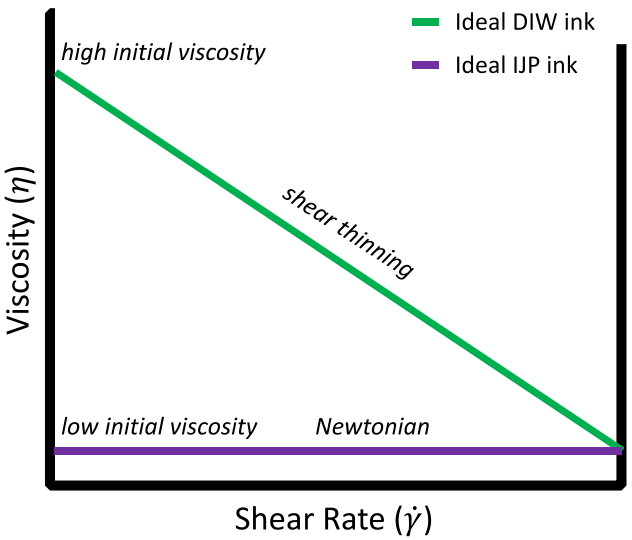

FIGURE 6 Ideal rheology of DIW and IJP inks. Suitable inks for IJP display Newtonian behavior with low initial viscosities. Inks typically utilized within DIW processes display shear-thinning behavior and have high initial viscosities. The shear-thinning curve here is intended to serve as a conceptual aid to demonstrate the decrease in viscosity with increasing shear rate. The shape of the shear-thinning curve can vary depending on materials, solvents, or concentrations. [Color figure can be viewed at wileyonlinelibrary.com]

manner with a curing step in between layers. If the ink has a relatively high initial viscosity, then the ability of the ink to retain its shape after exiting the nozzle can allow for continuous printing without the need for a curing step between layers. Desired ink rheologies can be achieved through clever molecular design of polymer side chains.[36] Most of the inks currently being developed for DIW systems utilize shear-thinning dispersions or pastes to achieve high shape retention upon immediate exiting of the nozzle. This allows for shorter overall printing times and higher resolution features via careful tuning of ink rheology. Another attractive feature of DIW systems is the deposition of material at relatively low temperatures (i.e., room temperature). This has allowed for the deposition of heat-sensitive materials such as CPs. In the following sections, we will highlight several recent reports where truly 3D structures containing CPs were created.

Rheological investigation and DIW printing of a polyaniline-based ink. As stated previously, suitable rheological properties are of paramount importance when developing a DIW platform. Work carried out at the University of Western Ontario under the direction of Prof. Aaron D. Price tackled this problem directly for the case of polyaniline (PANI).[37] PANI is a prototypical conducting polymer and can exist as three distinct oxidation states, of which only one displays good electrical conductivity upon acid doping, referred to as the *emeralidine salt*.[38] The emeralidine salt is formed by reversible protonation of the partially oxidized form (emeralidine base) with strong protic acids (mineral acids, sulfonic acids, etc.).[39] Many groups have utilized formation of the salt to attenuate the physical properties of PANI via complexation with tailored counterions.[40–42] In this work, the team studied the complexation of dodecylbenzenesulfonic acid (DBSA) with PANI, and how the processing conditions affect final paste rheology and printing.[43]

To begin, the team took inspiration from previous work that had described doping of PANI with DBSA under different thermal conditions.[44] Using this work as a starting point, the team formed their inks via mechanical mixing of PANI and DBSA under different temperature/time regimes, and identified the suitable parameters to achieve the desired ink rheology: relatively high initial viscosities (η_0) and strong shear thinning.

In order to 3D print this ink, a DIW platform was built in-house from the combination of a commercially available FDM delta printer and a pneumatic extrusion system supplied by Nordson EFD. The printed specimen demonstrated that, while not exact, the extrusion pressure and print speed were predictive of the extruded line width. A number of different structures were successfully printed, including a bowl with a

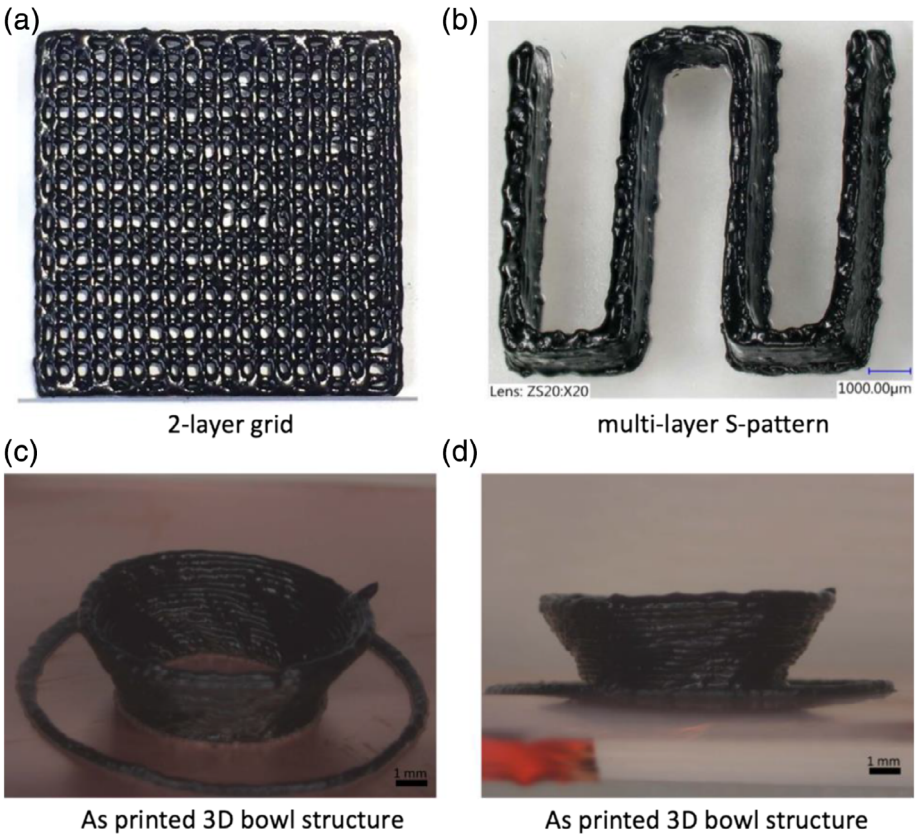

FIGURE 7 PANI–DBSA structures printed via a DIW process. (a,b) Example two-layer grid and multilayer S-pattern printed out of conductive PANI ink. (c,d) Bowl structure with 58° overhang angle successfully printed with conductive PANI-based ink. (Reproduced from 36, with permission from IOP Publishing.) [Color figure can be viewed at wileyonlinelibrary.com]

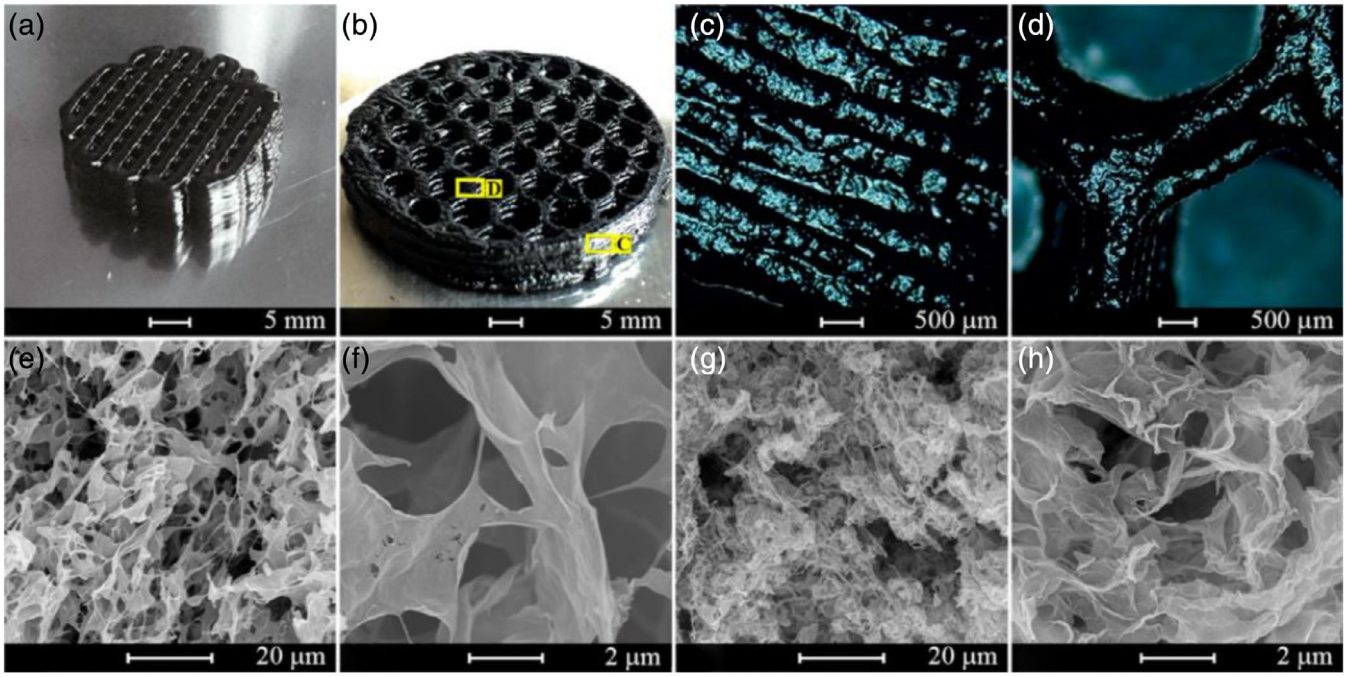

FIGURE 8 3D printed $PANI_{0.4}$/GO workpieces and their structure. (a) Column lattice formed by orthogonal lines layer by layer. (b) Honeycomb. (c,d) Micrographs of the surface of the honeycomb in (b). (e–h) Scanning electron microscopy (SEM) images of lyophilized $PANI_{0.4}$/GO workpiece (e,f) and lyophilized $PANI_{0.4}$/reduced GO (rGO) workpiece (g,h). (Reproduced from ref. 45, with permission from the American Chemical Society.) [Color figure can be viewed at wileyonlinelibrary.com]

challenging 58° overhang angle (Fig. 7). The printed structures are shown to be indeed conductive, but the electrical properties were not specifically quantified.[45] Overall, this initial report by the team shows the promise of developing robust, printed devices made from PANI. Further development of the ink and extrusion printer could lead to complex structures with the resolution necessary for incorporation in devices or multimaterial systems.

DIW printing of a PANI–graphene oxide composite. Research led by Hua Bai at Xiamen University recently disclosed the printing of conducting polymer-based composite inks. Their ink formulation contained a mixture of PANI and graphene oxide (GO) dispersed in *N*-methylpyrrolidone/water.[46] Tuning the relative composition of PANI to GO was proven to be the key to realizing optimal rheological properties for successful DIW printing. Inks with low PANI content underwent smooth extrusion but had a tendency to flow and not retain its shape well after exiting the nozzle, while those with high PANI content were prone to clogging during extrusion. Ink containing 40% PANI ($PANI_{0.4}$/GO) allowed for smooth extrusion and good shape retention, and was used for printing. Importantly, the resulting inks displayed higher viscosity than the precursor solutions (PANI and GO) viscosities, indicating the formation of a 3D network between PANI and GO. This was further supported by a dramatic increase in the storage modulus of the combined inks. This robust gel network is believed to originate from strong π–π interactions at the PANI/GO interface.

A three-step procedure is required to produce 3D PANI/GO structures with good electrical properties. The first step is deposition of the ink using a homemade 3D printer, extruded by a pneumatic syringe dispenser, into the desired 3D architecture. Next, this object is placed into a bath of hydroiodic acid to promote the reduction of the GO to rGO, which displays better electrical properties compared to its oxidized counterpart. Finally, dialysis of the remaining acid and salts using water and ethanol produced the desired structure. Examples of some of the printed structures and microscopic analysis are shown in Figure 8. A resolution of 300 μm was achieved utilizing their system. The equivalent series resistance of the composite was measured as 0.808 Ω via electrochemical impedance spectroscopy (EIS), demonstrating good electrical conductivity for the material. Using this ink and processing method, interdigitated planar supercapacitor was created with a H_2SO_4/poly(vinyl alcohol) gel electrolyte. The supercapacitor has an areal specific capacitance of 1255 ± 74 mF cm^{-2} at a current density of 4.2 ± 0.8 mA cm^{-2}, much higher than other supercapacitors prepared via DIW.[47–49]

DIW of poly(3,4-ethylene dioxythiophene):poly(styrene sulfonate) within a biopolymer film. A team led by Marc in het Panhuis at the University of Wollongong has detailed the extrusion of a poly(3,4-ethylene dioxythiophene):poly(styrene sulfonate) (PEDOT:PSS) paste onto different substrates in a recent report.[50] While this report only describes the creation of 2D structures, it is notable for their fundamental examination of the substrate's effect on the extruded tracks. A PEDOT:

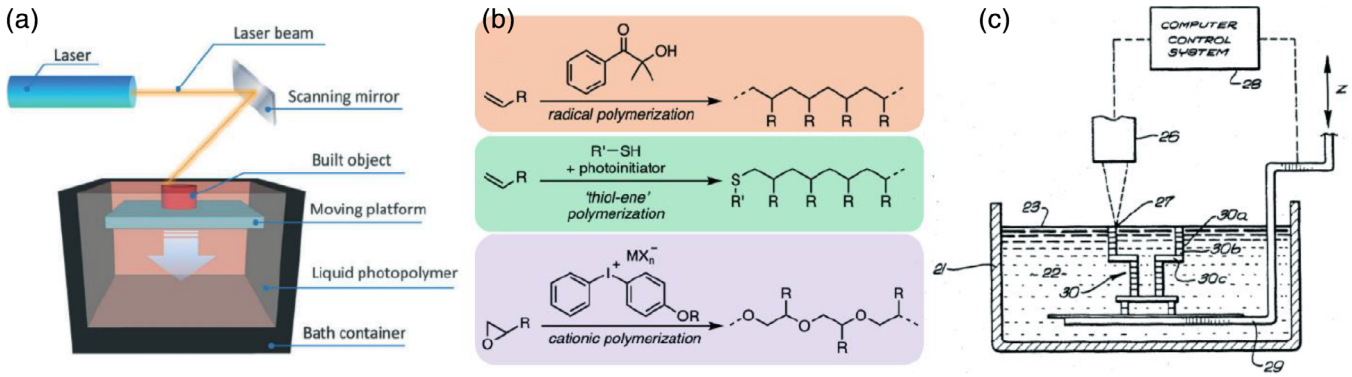

FIGURE 9 (a) Schematic diagram of the typical SLA process with specific parts annotated. (b) Chemistries commonly employed in photopolymer resins including radical, thiol–ene, and cationic polymerizations. (c) Schematic of the SLA process as described in Chuck Hull's original patent. [Part (a) reproduced from ref. 57, with permission from the Royal Society of Chemistry, part (c) reproduced from ref. 15.] [Color figure can be viewed at wileyonlinelibrary.com]

PSS paste with a suitably high initial viscosity and shear-thinning behavior is first developed. Utilizing a pneumatic syringe, the authors printed lines of PEDOT:PSS and investigated the influence of two different substrates, glass and a hydrogel made of chitosan and hyaluronic acid, on the electrical properties of the extruded material. They found that tracks printed on the surface of the glass or hydrogel had lower conductivities (6.3 and 1.7 S cm^{-1}) then tracks printed within the hydrogel (17 S cm^{-1}). The authors believe that this difference in conductivity most likely originates from the evaporation of water from the PEDOT printed on surface compared to the hydrated track suspended within the gel. This work is of note as one of the only reports that attempts to directly process a benchmark CP, PEDOT:PSS, using the DIW technique and investigated the structure–property relationships to some extent. While the authors have currently demonstrated 2D printing, the technique used to suspend printed tracks in a gel can be readily transformed to construct 3D structures by constructively stacking lines on top of one another. The gel medium can provide the structural support for the embedded 3D structures. Such matrix-stabilized 3D printing for soft materials has been demonstrated by the groups of Prof. Alshakim Nelson and Prof. Adam Feinberg.[51,52]

Direct writing of PEDOT:PSS micropillar arrays. Recent work carried out under the direction of Jadranka Travas-Sejdic at the University of Auckland described the formation of PEDOT:PSS micropillar arrays using an electrochemical DIW technique.[53] This work builds upon an earlier report by the group demonstrating a similar technique for the deposition of polypyrrole (PPY).[54] The current method operates using a glass micropipette, with a narrow inner diameter of roughly 2–20 μm, that contains a Pt wire as an electrode. A solution of PEDOT:PSS containing high boiling solvents (dimethyl sulfoxide, ethylene glycol) and a crosslinking agent ((3-glycidlyoxypropyl)-trimethoxysilane) is infiltrated into the barrel of the micropipette. The micropipette is lowered, using a piezoelectric, to a substrate containing an Au counter electrode to which a bias voltage (0.5 V) is applied. Upon contact of the solution to the metallic substrate, a significant current is generated and the tip is raised at a constant rate (typically 1–2 μm s^{-1}) leaving behind a solid PEDOT:PSS micropillar. Investigation using Raman spectroscopy confirmed the integrity of the PEDOT polymer within the structures. These micropillars can be patterned into arrays and show good electrochemical stability with no significant degradation after 100 cyclic voltammetry cycles. They are also mechanically robust, recovering immediately after manipulation using the tip. Using this technique, the group was able to print micropillars with extremely large aspect ratios of nearly 700×. While the authors only describe the creation of pillars, their work highlights the resolution that DIW could achieve using custom-made nozzles with micrometer-sized diameters. Furthermore, the prospect of printing narrow lines in the direction perpendicular to the substrate is of significant importance for electronic applications. Devices with vertically stacked structures can maximize device density while minimizing the size of the electronics. The ability to print via interconnects in the direction perpendicular to the device planes that join all the stacked layers can enable many new opportunities.

Outlook for DIW of CPs. The creation of 3D structures incorporating CPs via DIW is still in its infancy. The current focus remains on the development of printable inks that incorporate CPs and fabricating structures without sacrificing their electrical properties. In two of the reviewed studies, careful development of ink rheology was critical to successful printing. The major advantage of applying the DIW technique to CPs is its high versatility in printing pastes that can be generated from virtually any solution processible material including CPs. While the majority of inks currently developed have focused on PANI and PEDOT:PSS, careful synthetic design of monomers, side chains, and selection of additives can allow for inks with other CPs that have desired electronic, electrical, optical, and mechanical properties. One current limitation is that the interior of commercially available extruders typically contains polymers that are sensitive to acid and organic solvents,

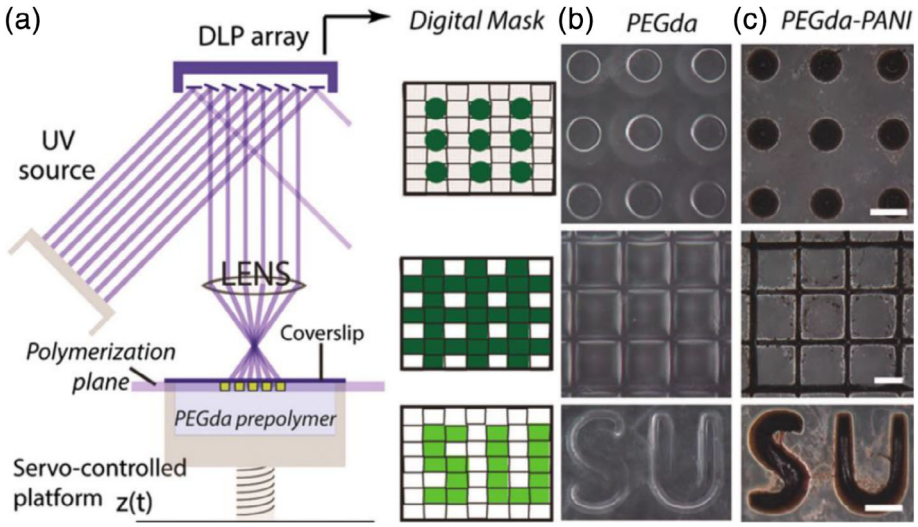

FIGURE 10 Design-driven fabrication approach to develop PEGda-PANI samples: (a) schematic of projection stereolithography process. PEGda monomer solution is placed in a chamber covered by a methacrylated glass coverslip. Computer aided design files were used to generate a series of virtual masks (dot, grid, and letter patterns). Polymerization of the 3D scaffold begins at the coverslip surface, where UV light modulated by DLP array is focused. (b,c) Crosslinked PEGda and PEGda–PANI microstructures adhered to silanized glass coverslip are visualized using HIROX instrument. All scale bars are 200 μm. (Reproduced from ref. 61, with permission from the Royal Society of Chemistry.) [Color figure can be viewed at wileyonlinelibrary.com]

severely limiting the types of fluids that can be utilized. This could be overcome with the development of extruders made out of resistant materials like polypropylene or Teflon. Such improvement in chemical compatibilities can potentially enable the printing of CP hydrogels and organogels already reported in literature.[55,56] These limitations aside, with the low-cost to entry and high versatility that DIW offer, the CP field is sure to see a wealth of studies on DIW-based processing in the near future.

Next, we will review the printing of CPs via vat photopolymerization, an AM approach with its own unique advantages and challenges.

Vat Photopolymerization Techniques: SLA and DLP

Vat photopolymerization is an AM technique in which a solid structure is produced from a pool of liquid resin, typically a mixture of monomers, oligomers, and photoinitiators. The two most commonly used methods are SLA and DLP. While SLA and DLP differ in the radiation source, either a laser or a LED projector, the actual printing method is identical in both techniques. A build plate is used to create a narrow layer of resin (typically ≤100 μm) which is hardened through exposure to a specific wavelength of light. The hardening of successive layers creates a 3D structure with high dimensional freedom and accuracy. SLA and DLP systems are available that build in either a top-down or bottom-up fashion. Exposure of the resins to light promotes decomposition of a photoinitiator which generates reactive species and initiates chemical reactions for solid polymer formation [Fig. 9(a)]. To date, nearly all resins utilize some combination of radical, cationic, or thiol–ene type mechanisms to crosslink and strengthen the resulting polymer structure [Fig. 9(b)].[19] Although SLA/DLP can seem complicated when compared to DIW, principally due to the need to develop chemical strategies, there are significant advantages to this approach. One major advantage of vat polymerization is the resolution that can be achieved. Whereas common DIW extruders struggle to reach resolution below 100 μm without specialty machined tips, this resolution can be effectively achieved even with hobbyist SLA/DLP equipment.[57,58] Also, SLA/DLP are capable of producing complex, porous structures by using the uncured resin as a support bath for the growing part. Another advantage is speed, where techniques such as DLP can create an entire 2D layer of the print at the same time, dramatically shortening overall print time.

The incorporation of CPs in SLA and DLP methodologies has seen relatively few reports so far. This is likely due to a number of fundamental obstacles that must be overcome when combining these two fields. First and foremost is the overlapping UV–visible absorbances of the growing CPs and the photoinitiator utilized to catalyze their formation.[59] CPs usually absorb intensely in the UV and visible region due to the presence of long chains of conjugated π bonds, which provide them with their electrically conductive properties.[60] This can pose a balancing act in the design of a system where the produced conducting polymer does not disrupt, or inhibit, subsequent layer curing by outcompeting the photoinitiator for the incident photons. Also, CPs can have quite complex redox chemistries which may be incompatible with the reactive species formed during classic photoinitiator decomposition, that is, radicals. Yet, despite these caveats, a number of groups have developed strategies to successfully grow structures containing CPs using SLA and DLP.

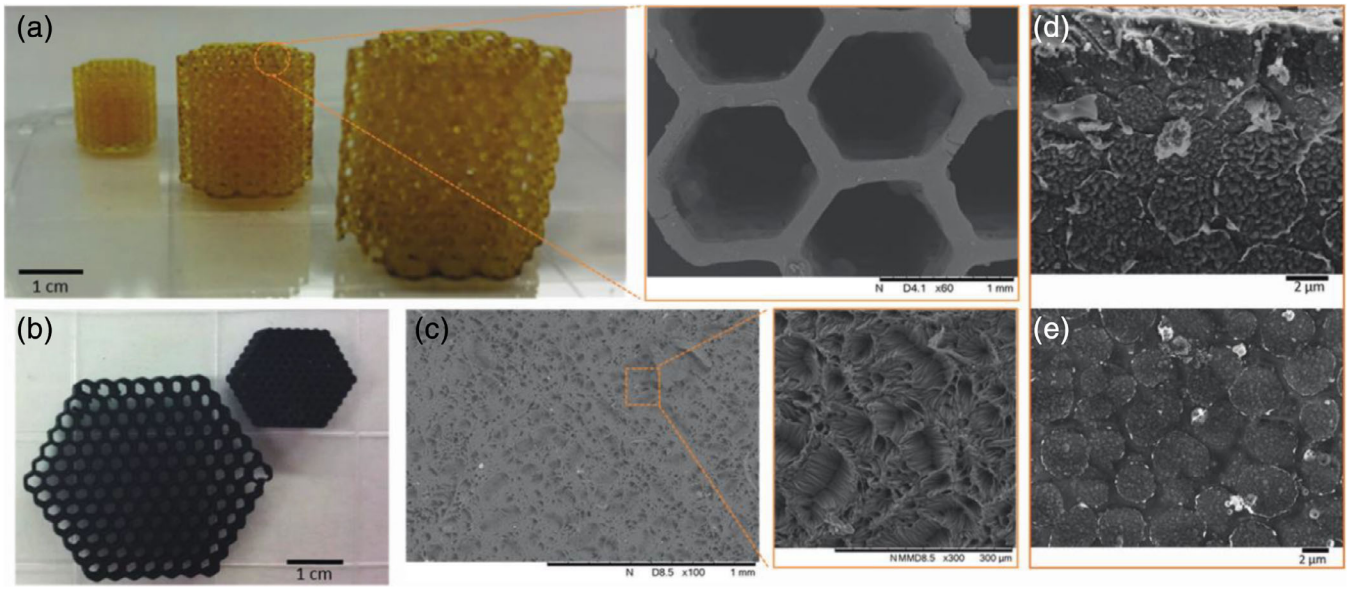

FIGURE 11 (a) Example of a honeycomb structure printed in different dimension and SEM detail of the features obtained. (b) 3D printed PEGda–PPY honeycomb structures. (c) SEM images of the PPY surface. (d,e) Cross section of a thick sample (4 mm). (Reproduced from ref. 63, with permission from John Wiley and Sons.) [Color figure can be viewed at wileyonlinelibrary.com]

As we have described, a combined strategy of (a) understanding the photochemical properties of CPs as well as (b) modification of contemporary SLA/DLP strategies could enable the successful application of SLA/DLP to CPs. Clever chemistries can enable the successful formation of CPs using the input of light. More broadly, the creation of CPs using the input of light as a stimulus has a rich history and is the subject of a recent review.[61] This can also allow for multimaterial parts, containing conductive and structural elements, if suitably orthogonal chemistries could be developed. In the following sections, we will describe recent work to unify the strategies listed above to realize the printing of 3D structures containing CPs via the input of light. The methods employed fall into two broad categories, (a) the formation of a support structure using SLA/DLP and the subsequent growth of a CP in a separate step and (b) the direct growth of a CP during the SLA/DLP process.

Postprinting growth of CPs within SLA/DLP-grown structures. To date, a number of groups have reported on the successful growth of CPs within 3D printed hydrogels in a separate postprinting step. Recently, the group of Pranav Soman at Syracuse University developed an interfacial polymerization approach to the synthesis of conductive PANI within poly(ethylene-glycol) diacrylate (PEGda) or gelatin methacrylate (GelMA) gels (Fig. 10).[62] Their process begins with the formation of a crosslinked hydrogel utilizing a home-built DLP setup. After printing, the gel is placed in DI water to remove any unreacted monomers or photoinitiators. The washed gel is then placed in a solution of ammonium persulfate (APS) in 1 M HCl to allow for diffusion of the APS into the gel network. After the gel has reached equilibrium, it is transferred to a solution of aniline in hexanes and rapidly changes colors as conductive PANI grows within the gel. The use of two immiscible solvents (water and hexanes) allows for the confinement of the polymerization solely within the gel as the absorbed APS cannot diffuse out of the hydrogel and into the hexanes solution.

Subsequent testing of the PEGda-PANI hydrogel confirmed that the incorporation of PANI had no effect on the compression modulus of the gel and that they were indeed electrically conductive. Conductive gel patterns with small features around 100 μm were produced using this approach. In a subsequent report by this research group, this methodology was expanded to create GelMA–PANI hydrogels using a similar strategy.[63] In that system, the authors found that the addition of the conductive PANI network led to worse charge transport characteristics, most likely due to the inhibition of ion-diffusion throughout the gel. Interestingly, EIS showed that at lower, physiologically relevant frequencies, the GelMA–PANI network displayed lower impedance values as compared to just GelMA, with lower resistances values overall for the gels with conductive PANI networks.

Also utilizing an interfacial polymerization approach, the group of Jun Yang at the University of Western Ontario reported the growth of PPY within 3D-printed PEGda networks (Fig. 11).[64] In their work, they utilized a commercial DLP printer to produce complex PEGda hydrogels. Subsequent soaking of these hydrogels in an aqueous solution of $FeCl_3$ followed by a solution of pyrrole in cyclohexane promoted the growth of conductive PPY networks within the hydrogel. The incorporation of PPY led to an increase in the compressive Young's moduli of the resulting gels, and a dramatic decrease in the electrical resistance by an order of magnitude or more. These three reports highlight the creative approach the authors undertook to create conductive, 3D structures via

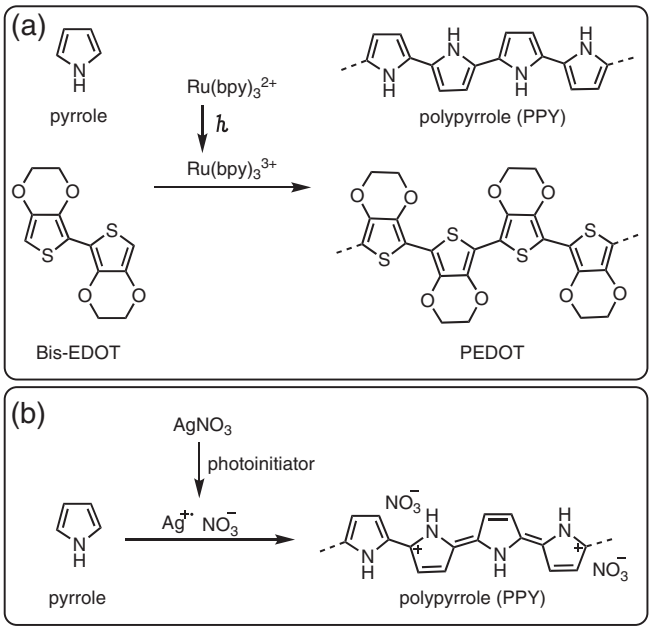

FIGURE 12 Synthesis of CPs via photogenerated oxidants. (a) Photogeneration of a ruthenium(III) oxidant can successfully initiate polymerization to form PPY and PEDOT.[66] (b) Radical sensitization of silver ions using photoinitiators can induce polymerization of pyrrole to PPY.[67]

initial printing of nonconductive, porous substrates. These approaches benefit from utilizing canonical monomers for the initial stereolithographic printing. As highlighted, complex structures can be reliably produced using well-understood chemistries. The downside to this process is the difficulty in achieving high loading of the electrical network within the porous gels. In the next section, we will describe a more direct approach to the synthesis of complex structures with the conductive network being formed concurrently during the printing process.

Direct synthesis of conducting polymers during SLA/DLP printing. Initial progress toward the direct printing of conductive 3D structures was reported under the direction of Junji Sone at Tokyo Polytechnic University in 2014.[65,66] In two reports, the authors described their approach to the

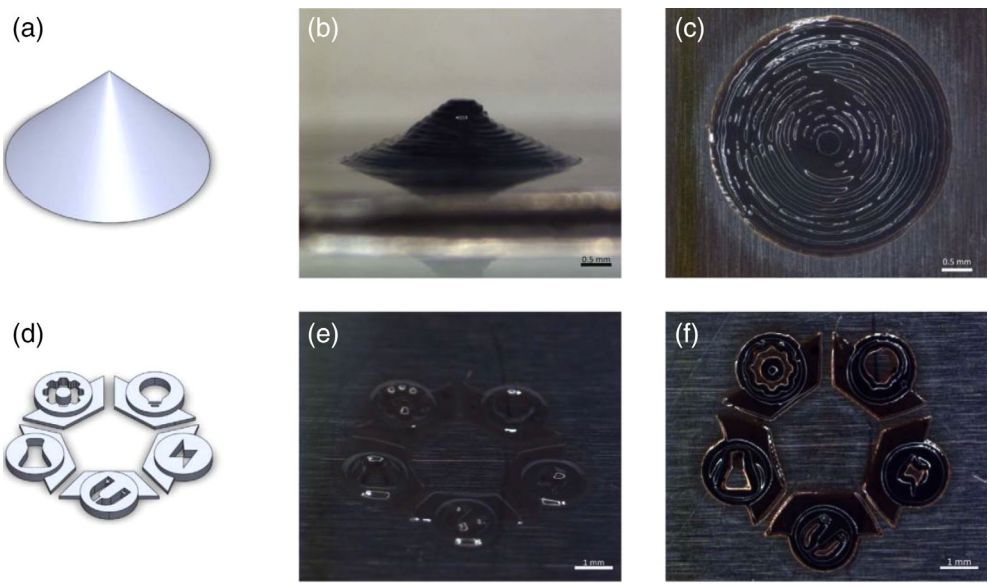

FIGURE 13 PPY containing conductive structures produced through DLP printing of a dual reactive resin. The structures contain a combination of a crosslinked diacrylate network and PPY network to lend mechanical strength and electrical conductivity respectively. (Reproduced from ref. 66, with permission from Elsevier.) [Color figure can be viewed at wileyonlinelibrary.com]

photochemical production of conductive PPY and PEDOT structures within a transparent polymer (Nafion) sheet [Fig. 12 (a)]. Their approach utilized a photoactive transition metal catalyst, tris(2,2′-bipyridyl) ruthenium(II) ($Ru(bpy)_3^{2+}$), acting as an oxidant after photoexcitation via its two photon-absorption using a femtosecond laser pulse. This approach relies on careful tuning of the redox interaction of the photo-oxidant and the monomers so that polymerization is effectively initiated. In the case of PPY, the oxidizing power of the $Ru(bpy)_3^{3+}$ was able to successfully initiate polymerization via direct oxidation of pyrrole monomers. In the case of PEDOT, 3,4-ethylenedioxythiophene (EDOT) monomers had an oxidation potential that was too high for $Ru(bpy)_3^{3+}$. To overcome this challenge, the authors found that the simple dimer of EDOT, bis-EDOT, had a lower oxidation potential that would drive electron transfer from bis-EDOT to the photocatalyst. This allowed for the successful creation of PEDOT structures utilizing the same photoredox catalyst. Having developed successful chemical systems for the production of PEDOT and PPY, the authors turned their attention to creating 3D structures. The photo reactive solutions were soaked into a Nafion polymer prior to excitation with the laser. Utilizing a piezoelectric stage with a focused femtosecond laser, they were able to successfully create structures with feature sizes down to 500 nm. Their process allowed for the creation of 3D structures with the major limitation being the confinement of the printing area to within the Nafion film.

Recently, the first report of the synthesis of a CP concurrently with the generation of a support structure was published. The work was carried out under the direction of Aaron D. Price at Western University in Ontario.[67,68] The authors describe the development of a divergent catalytic system originating from a single photoinitiator. Photopolymerization of pyrrole within films had been described in the literature but was never incorporated into an AM system.[69] In their setup, a UV-absorbing photoinitiator creates radical centers that promote polymerization of a diacrylate support structure, while also oxidizing silver ions that initiate the polymerization of pyrrole [Fig. 12(b)]. This process led to a solid, black, conductive structures in a single printing operation using a DLP printer (Fig. 13). Spectroscopic analysis (Fourier transform infrared) lends support to the successful growth of PPY within the 3D printed structure. The conductivity of the DLP-printed PPY was as high as 5×10^{-2} S cm^{-1}, which is comparable to similar systems that have been reported.[70] This report represents a large step toward the direct formation of 3D CP structures using just light. Currently, the structures can only be produced utilizing a mixed resin employing canonical acrylate-based monomers to provide mechanical support. Within these structures, the electrical conductivity is low, most likely due to dilution of the conjugated network within the overall structure. If a photoactivated system could be developed to produce solely CP containing structures that were mechanically sound, this would be a major step toward producing 3D CPs with complete design freedom and good electrical properties. Future development of clever synthetic chemistries could make this a reality.

Outlook for SLA/DLP 3D printing of conducting polymers. In this section, we have provided an overview to recent work on 3D conductive structures containing CPs produced via an SLA/DLP process. With the recent proof-of-concept studies reviewed in this section, this area is ripe for a wealth of innovation in the coming years. The evolution of clever chemistries that allow for the controlled, rapid synthesis of CPs using light can provide a boon to the field.

OUTLOOK

To date, the application of 3D printing methods for processing CPs is still in its infancy. Recent work highlighted in this review has demonstrated proof-of-concept for achieving this outcome. In addition to the ability to create 3D freeform organic electronics, total 3D design freedom, the generation of little to no waste, and the combination of processing and device patterning in one-step are attractive features of this worthy goal. Therefore, it is evident that many exciting opportunities lie within this nascent field.

First, as the case for any new processing methods applied to a given class of material, thorough processing–structure–property relationships need to be investigated to develop a holistic evaluation of the benefits and limitations of this approach. The structure–property relationships of CPs that are heavily dependent on processing conditions include, but are not limited to, chain conformation, interchain packing arrangement, domain morphology, crystallinity, charge carrier mobility, and conductivity. The understanding of these fundamental properties and their relationship with processing conditions has fueled a phase of rapid growth in the molecular engineering and bespoke processing method developments for CPs. This research is largely responsible for the commercial success of OPV, OLEDs, and OFETs). We speculate the same progression will be necessary for the field of 3D printing of CPs to mature. Furthermore, current proof-of-concept studies have been focused on intrinsically conducting polymers. The field of semiconducting polymers remains untapped and full of opportunities.

With the understanding of these fundamental properties and relationships, researchers will have the toolbox to manipulate the processing methods to create new and enhanced properties. Development in two parallel fields will be required.

1. New chemistries for synthesizing or formulating CPs will have to be developed for existing 3D printing methods. For instance, viscosity-tuning additives that do not negatively affect physical properties, or side-chain chemistry that can induce gelation, are necessary for enabling DIW-based 3D printing for a wider range of CPs. New photochemical synthetic routes for CPs can initiate a chain of developments in the area of SLA/DLP printing. The recent pioneering work on melt-processed semiconducting polymers from Jianguo Mei's group at Purdue University[71,72] offers a hopeful glimpse to the prospect of 3D printing this class of materials using FDM or SLS-based approaches.

2. Tailored 3D printing tools need to be developed for processing CPs. This class of materials are typically highly acidic (i.e., many conducting polymers) or processed utilizing corrosive organic solvents (i.e., many semiconducting polymers), with which few commercially available 3D printers are chemically compatible. In-house machine building is currently a necessary component for 3D printing CPs. Chemically compatible commercial 3D printers will likely bring in researchers without tool building experience and accelerate the development of the field.

Finally, the drastic expansion of form factor, functionality, geometry, personalization, and total design freedom enabled by 3D printing is poised to positively impact a myriad of potential applications. They include, personalized organic wearable electronics and bioelectronics, arbitrarily shaped organic energy harvesting and storage devices, functional prosthetics, or soft robotics with embedded organic circuitry, just to name a few. Because of the design freedom of 3D printing, an artistic factor can also be readily attached to these functional devices, bringing the field one-step closer to infusing aesthetically pleasing and humanistic design into new cutting-edge technology.

We hope these exciting prospects can spark the interest of researchers in the CP community to join the rapidly growing 3D printing community, and the 3D printing community to add CPs as a class of lightweight, low cost, functional materials that are full of possibilities to their material repertoire.

ACKNOWLEDGMENTS

The authors thank John Misiaszek for assisting with TOC graphics. The authors are grateful for the help of Maria Celeste Castillo and Victor Hernandez with designing the journal cover. The authors would also like to acknowledge the University of California, Merced startup fund and the Gordon and Betty Moore Foundation for supporting this research.

REFERENCES AND NOTES

1 H. Shirakawa, E. J. Louis, A. G. MacDiarmid, C. K. Chiang, A. J. Heeger, *J. Chem. Soc. Chem. Commun.* **1977**, 579.

2 Press Release. https://www.nobelprize.org/prizes/chemistry/2000/press-release/

3 T. Swager, *Macromolecules* **2017**, *50*, 4867.

4 A. Moliton, R. C. Hiorns, *Polym. Int.* **2004**, *53*, 1397.

5 J. Chen, Y. Cao, *Acc. Chem. Res.* **2009**, *42*(11), 1709.

6 H. Sirringhaus, *Adv. Mater.* **2014**, *26*, 1319.

7 J. Mei, Z. Bao, *Chem. Mater.* **2014**, *26*, 604.

8 A. O. Patil, Y. Ikenoue, F. Wudl, A. J. Heeger, *J. Am. Chem. Soc.* **1987**, *109*, 1858.

9 S. Huang, Y. Liu, Y. Zhao, Z. Ren, C. F. Guo, *Adv. Funct. Mater.* **2019**, *29*(6), 1805924.

10 Y. Wang, C. Zhu, R. Pfattner, H. Yan, L. Jin, S. Chen, F. Molina-Lopez, F. Lissel, J. Liu, N. I. Rabiah, Z. Chen, J. W. Chung, C. Linder, M. F. Toney, B. Murmann, Z. Bao, *Sci. Adv.* **2017**, *3*(3), e1602076.

11 Y. Diao, L. Shaw, Z. Bao, S. C. B. Mannsfeld, *Energ. Environ. Sci.* **2014**, *7*, 2145.

12 A. Facchetti, *Chem. Mater.* **2011**, *23*, 733.

13 A. Sydney Gladman, E. A. Matsumoto, R. G. Nuzzo, L. Mahadevan, J. A. Lewis, *Nat. Mater.* **2016**, *15*, 413.

14 T. J. Wallin, J. Pikul, R. F. Shepherd, *Nat. Rev. Mater.* **2018**, *3*, 84.

15 C. W. Hull (UVP Inc.). U.S. Patent 4,575,300, March 11, **1986**.

16 P. J. Bártolo, I. Gibson, In *Stereolithography: Materials, Processes and Applications*; P. J. Bártolo, Ed.; Springer Science +Business Media, LLC, New York, **2011**.

17 H. Kodama, *Rev. Sci. Instrum.* **1981**, *52*(11), 1770.

18 M. Guvendiren, J. Molde, R. M. D. Soares, J. Kohn, *ACS Biomater Sci. Eng.* **2016**, *2*, 1679.

19 S. C. Ligon, R. Liska, J. Stampfl, M. Gurr, R. Mülhaupt, *Chem. Rev.* **2017**, *117*, 10212.

20 B. C. Gross, J. L. Erkal, S. Y. Lockwood, C. Chen, D. M. Spence, *Anal. Chem.* **2014**, *86*, 3240.

21 L. M. Leung, Handbook of Thermoplastics. In ; O. Olabisi, K. Adewale, Eds.; Taylor & Francis: Boca Raton, FL, **2015**, Chapter 20, p. 669.

22 M. Jørgensen, K. Norrman, F. C. Krebs, *Sol. Energ. Mater. Sol. C* **2008**, *92*, 686.

23 B. Louis, S. Caubergh, P.-O. Larsson, Y. Tian, I. G. Scheblykin, *Phys. Chem. Chem. Phys.* **2018**, *20*, 1829.

24 Z. Hu, B. Shao, G. T. Geberth, D. A. Vanden Bout, *Chem. Sci.* **2018**, *9*, 1101.

25 C. Wang, H. Dong, W. Hu, Y. Liu, D. Zhu, *Chem. Rev.* **2012**, *112*, 2208.

26 A. T. Cullen, A. D. Price, *Smart Mater. Struct.* **2019**. *28*, 104007.

27 P. Clavert, *Chem. Mater.* **2001**, *13*, 3299.

28 A. Teichler, J. Perelaer, U. S. Schubert, *J. Mater. Chem. C* **2013**, *1*, 1910.

29 M. Gao, L. Li, Y. Song, *J. Mater. Chem. C* **2017**, *5*, 2971.

30 B. Yoon, D.-Y. Ham, O. Yarimaga, H. An, C. W. Lee, J.-M. Kim, *Adv. Mater.* **2011**, *23*, 5492.

31 M. Chang, G. T. Lim, B. Park, E. Reichmanis, *Polymers* **2017**, *9*, 212.

32 T. Rödlmeier, T. Marszalek, M. Held, S. Beck, C. Müller, R. Eckstein, A. J. Morfa, R. Lovrincic, A. Pucci, U. Lemmer, J. Zaumseil, W. Pisula, G. Hernandez-Sosa, *Chem. Mater.* **2017**, *29*, 10150.

33 J. Cesarano, T. A. Baer, P. Calvert, Recent Developments in Freeform Fabrication of Dense Ceramics From Slurry Deposition, Proceedings of the Solid Freeform Fabrication Symposium, Austin, TX. **1997**, 25–32.

34 J. A. Lewis, *Adv. Funct. Mater.* **2006**, *16*, 2193.

35 S. Turunen, S. Kaisto, I. Skovorodkin, V. Mironov, T. Kalpio, S. Vainio, A. Rak-Raszewska, *AIMS Cell Tissue Eng.* **2018**, *2*, 119.

36 M. Abbasi, L. Faust, M. Wilhelm, *Adv. Mater.* **2019**, *31*, 1806484.

37 F. B. Holness, A. D. Price, *Smart Mater. Struct.* **2018**, *27*, 015006.

38 M. Angelopoulos, G. E. Asturias, S. P. Ermer, A. Ray, E. M. Scherr, A. G. Macdiarmid, M. Akhtar, Z. Kiss, A. J. Epstein, *Mol. Cryst. Liq. Cryst.* **1988**, *160*, 151.

39 J.-C. Chiang, A. G. MacDiarmid, *Synth. Met.* **1986**, *13*, 193.

40 J. E. Yoo, J. L. Cross, T. L. Bucholz, K. S. Lee, M. P. Espe, Y.-L. Loo, *J. Mater. Chem.* **2007**, *17*, 1268.

41 J. A. Syed, S. Tang, H. Lu, X. Meng, *Ind. Eng. Chem. Res.* **2015**, *54*, 2950.

42 Y. Xia, J. M. Wiesinger, A. G. MacDiarmid, A. J. Epstein, *Chem. Mater.* **1995**, *7*, 443.

43 G. I. Titelman, M. Zilberman, A. Siegmann, Y. Haba, M. Narkis, *J. Appl. Polym. Sci.* **1997**, *66*, 2199.

44 M. Zilberman, G. I. Titelman, A. Siegmann, Y. Haba, M. Narkis, D. Alperstein, *J. Appl. Polym. Sci.* **1997**, *66*, 243.

45 F. B. Holness, Additive Manufacturing Process of 3D Polyaniline Transducers via Direct Ink Writing, M.E.S. Thesis, University of Western Ontario, London, Canada, September **2017**.

46 Z. Wang, Q. Zhang, S. Long, Y. Luo, P. Yu, Z. Tan, J. Bai, B. Qu, Y. Yang, J. Shi, H. Zhou, Z. Y. Xiao, W. Hong, H. Bai, *ACS Appl. Mater. Interfaces* **2018**, *10*, 10437.

47 C. Zhu, T. Liu, F. Qian, T. Y. Han, E. B. Duoss, J. D. Kuntz, C. M. Spadaccini, M. A. Worsley, Y. Li, *Nano Lett.* **2016**, *16*, 3448.

48 B. L. Chen, Y. Z, X. H. Jiang, Y. Tang, Y. Pan, S. Hu, *ACS Appl. Mater. Interfaces* **2017**, *9*, 28433.

49 W. Yu, H. Zhou, B. Q. Li, S. Ding, *ACS Appl. Mater. Interfaces* **2017**, *9*, 4597.

50 C. A. Mire, A. Agrawal, G. G. Wallace, P. Calvert, M. in het Panhuis, *J. Mater. Chem.* **2011**, *21*, 2671.

51 A. Basu, A. Saha, C. Goodman, R. T. Shafranek, A. Nelson, *ACS Appl. Mater. Interfaces* **2017**, *9*(46), 40898.

52 T. J. Hinton, Q. Jallerat, R. N. Palchesko, J. H. Park, M. S. Grodzicki, H.-J. Shue, M. H. Ramadan, A. R. Hudson, A. W. Feinberg, *Sci. Adv.* **2015**, *1*(9), e1500758.

53 P. Zhang, N. Aydemir, M. Alkaisi, D. E. Williams, J. Travas-Sejdic, *ACS Appl. Mater. Interfaces* **2018**, *10*, 11888.

54 N. Aydemir, J. Parcell, C. Laslau, M. Nieuwoudt, D. E. Williams, J. Travas-Sejdic, *Macromol. Rapid Commun.* **2013**, *34*, 1296.

55 F. Zhao, Y. Shi, L. Pan, G. Yu, *Acc. Chem. Res.* **2017**, *50*, 1734.

56 J. Y. Oh, S. Kim, H.-K. Baik, U. Jeong, *Adv. Mater.* **2016**, *28* (22), 4564.

57 R. B. Rao, K. L. Krafcik, A. M. Morales, J. A. Lewis, *Adv. Mater.* **2005**, *17*, 289.

58 A. Ambrosi, M. Pumera, *Chem. Soc. Rev.* **2016**, *45*, 2740.

59 H. Meier, U. Stalmach, H. Kolshorn, *Acta Polym.* **1997**, *48*, 379.

60 K. J. Wynne, G. B. Street, *Ind. Eng. Chem. Prod. Res. Dev.* **1982**, *21*, 23.

61 H. R. Heydarnezhad, B. Pourabbas, M. Tayefi, *Polym. Plast. Technol.* **2018**, *57*, 1093.

62 Y. Wu, Y. X. Chen, J. Yan, S. Yang, P. Dong, P. Soman, *J. Mater. Chem. B* **2015**, *3*, 5352.

63 Y. Wu, Y. X. Chen, J. Yan, D. Quinn, P. Dong, S. W. Sawyer, P. Soman, *Acta Biomater.* **2016**, *33*, 122.

64 E. Fantino, I. Roppolo, D. Zhang, J. Xiao, A. Chiappone, M. Castellino, Q. Guo, C. F. Pirri, J. Yang, *Macromol. Mater. Eng.* **2018**, *303*, 1700356.

65 K. Yamada, Y. Yamada, J. Sone, *Thin Solid Films* **2014**, *554*, 102.

66 K. Yamada, M. Watanabe, J. Sone, *Opt. Rev.* **2014**, *5*, 679.

67 A. T. Cullen, A. D. Price, *Synth. Met.* **2018**, *235*, 34.

68 A. T. Cullen, Fabrication of 3D Conjugated Polymer Structures via Vat Polymerization Additive Manufacturing, M.E.S. Thesis, University of Western Ontario, London, Canada, May **2018**.

69 A. W. Rinaldi, M. H. Kunita, M. J. L. Santos, E. Radovanovic, A. F. Rubira, E. M. Girotto, *Eur. Polym. J.* **2005**, *41*, 2711.

70 R. Nazar, S. Ronchetti, I. Roppolo, M. Sangermano, R. M. Bongiovanni, *Macromol. Mater. Eng.* **2015**, *300*, 226.

71 Y. Zhao, X. Zhao, M. Roders, A. Gumyusenge, A. L. Ayzner, J. Mei, *Adv. Mater.* **2017**, *29*, 1605056.

72 Y. Zhao, A. Gumyusenge, J. He, G. Qu, W. W. McNutt, Y. Long, H. Zhang, L. Huang, Y. Diao, J. Mei, *Adv. Funct. Mater.* **2018**, *28*, 1705584.